The Mechanisms of Protonation of $[M(\eta^5\text{-}C_5H_5)_2H_2]$ (M = Mo or W)†

Richard A. Henderson* and Kay E. Oglieve
Agricultural and Food Research Council, Institute of Plant Science Research, Nitrogen Fixation Laboratory, University of Sussex, Brighton BN1 9RQ, UK

The reaction between $[M(\eta^5\text{-}C_5H_5)_2H_2]$ (M = Mo or W) and an excess of anhydrous HCl occurs by essentially the same mechanism for the two complexes. Protonation of the tungsten complex involves initial attack at a hydride ligand to generate the spectroscopically detected $[W(\eta^5\text{-}C_5H_5)_2H(\eta^2\text{-}H_2)]^+$, which subsequently undergoes an intramolecular oxidative cleavage of the dihydrogen ligand to give the trihydride, $[W(\eta^5\text{-}C_5H_5)_2H_3]^+$. The kinetic and thermodynamic isotope effects associated with these elementary reactions have been determined. Protonation of the analogous molybdenum complex also involves initial attack at a hydride ligand. However, in this system kinetic and spectroscopic studies indicate that the subsequent cleavage of the dihydrogen ligand to form $[Mo(\eta^5\text{-}C_5H_5)_2H_3]^+$ occurs *via* the rapid formation of a detectable binuclear species which is probably $[\{Mo(\eta^5\text{-}C_5H_5)_2H_2\}_2(\mu\text{-}H)]^+$.

We are interested in defining the details of protonation of transition-metal complexes, especially those containing co-ordinated small molecules such as hydrides, dinitrogen and unsaturated hydrocarbons.[1] In particular we want to understand the factors which discriminate between protonation at the metal or the ligand, and the consequences of such attack at these two types of sites in terms of any product subsequently released.[2]

Probably the simplest ligand capable of protonation is a hydrido group to give a co-ordinated dihydrogen species. Since the first isolation of thermally stable dihydrogen complexes,[3] it has become clear that such species may be detected as transient species on the pathway which results, ultimately, in a classical hydride, Fig. 1.

There have been several claims[4–7] that hydride ligands are preferentially attacked by protons, however these studies are complicated by the possibility that the dihydrogen species results from initial formation of a dihydride which subsequently rearranges to give the dihydrogen complex. In order to circumvent this ambiguity we have adopted the strategy of studying the mechanisms of protonation of hydrido complexes using rapid reaction techniques to detect transient dihydrogen intermediates. In this context, we have recently shown[8] that the protonation of $[WH_4(PMePh_2)_4]$ produces $[WH_3(\eta^2\text{-}H_2)(PMePh_2)_4]^+$ initially, which subsequently rearranges to yield $[WH_5(PMePh_2)_4]^+$. Kinetic analysis of this system is complicated by intramolecular rearrangements of the polyhydrido-intermediate as shown in equation (1).

$$[WH_3(\eta^2\text{-}H_2)(PMePh_2)_4]^+ \rightleftharpoons [WH(\eta^2\text{-}H_2)_2(PMePh_2)_4]^+ \quad (1)$$

In this paper we report studies on the reactions of $[M(\eta^5\text{-}C_5H_5)_2H_2]$ (M = Mo or W) with anhydrous HCl in thf (tetrahydrofuran) shown in equation (2).

$$[M(\eta^5\text{-}C_5H_5)_2H_2] + HCl \rightleftharpoons [M(\eta^5\text{-}C_5H_5)_2H_3]^+\cdot Cl^- \quad (2)$$

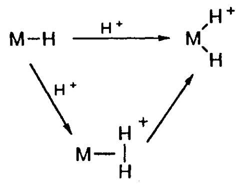

Fig. 1

For these systems the reactants and products are apparently 'classical' polyhydrides.[9–13] However, we now demonstrate that dihydrogen complexes are intermediates in these reactions. In addition, the simplicity of the tungsten system and the kinetic detail we can obtain therefrom allows us to define the isotope effects associated with the formation of the dihydrogen complex and its subsequent rearrangement to give the trihydride. The analogous molybdenum system also involves a transient dihydrogen species, but this intermediate rapidly forms a binuclear species prior to rearrangement and cleavage to give the product, $[Mo(\eta^5\text{-}C_5H_5)_2H_3]^+$.

Experimental

All manipulations were routinely performed under an atmosphere of dinitrogen using Schlenk or syringe techniques as appropriate. The complexes $[M(\eta^5\text{-}C_5H_5)_2H_2]$ (M = Mo[9] or W[10]) were prepared by the literature methods and purified by sublimation *in vacuo*. The isolated materials gave satisfactory elemental analyses (Found: C, 52.6; H, 5.1. Calc. for $C_{10}H_{12}Mo$: C, 52.6; H, 5.3. Found: C, 38.0; H, 3.9. Calc. for $C_{10}H_{12}W$: C, 37.7; H, 3.8%), and ^1H and ^{13}C NMR spectra (see Results and Discussion).

The solvent, thf, was freshly distilled from sodium–benzophenone under an atmosphere of dinitrogen, immediately prior to use. Stock solutions of anhydrous HCl were prepared by mixing equimolar proportions of $SiMe_3Cl$ and MeOH in thf. Solutions of the acid for the kinetic studies were prepared by the necessary dilutions of a stock solution of anhydrous HCl, and were used within 1 h of preparation. Solutions of DCl were prepared in an analogous fashion from $SiMe_3Cl$ and MeOD. The ionic strength of the reaction was maintained at 0.1 mol dm^{-3} using $[NBu^n_4]BF_4$.

The kinetics were studied on a Hi-Tech SF51 stopped-flow spectrophotometer modified to handle air-sensitive solutions,

---

† *Supplementary data available* (No. SUP 56965, 5 pp.): rate constants and equilibrium constants for the reaction of $[W(\eta^5\text{-}C_5H_5)_2H_2]$ and anhydrous HCl and rate constants for the reaction of $[Mo(\eta^5\text{-}C_5H_5)_2H_2]$ and anhydrous HCl.

and interfaced to a Viglen computer *via* an A/D converter. The reactions were studied at 25.0 ± 0.1 °C maintained by a Grant LE8 thermostat tank. The reactions were studied by monitoring the absorbance changes associated with $[M(\eta^5\text{-}C_5H_5)_2H_2]$ in the range λ 340–600 nm. For M = W, the absorbance–time curves were exponential at all wavelengths (Fig. 2), and were analysed by computer program fits to a single exponential, which gave excellent fits to the data for greater than three half-lives. The rate constants thus determined were independent of the wavelength of study. For M = Mo, the absorbance–time profile is biphasic, consisting of an initial absorbance increase followed by an absorbance decrease to give the product (Fig. 7). The kinetics of the initial phase were analysed for a second-order dependence on the concentration of $[Mo(\eta^5\text{-}C_5H_5)_2H_2]$ from the usual graph of $([Mo]_t^{-1} - [Mo]_\infty^{-1})$ against time. The straight lines thus obtained were linear for greater than 70% of the reaction (Fig. 9). The second phase of the reaction between $[Mo(\eta^5\text{-}C_5H_5)_2H_2]$ and HCl were analysed as exponential curves by computer fits; the fits were excellent for at least three half-lives.

All kinetics were studied under conditions where [HCl]: $[M(\eta^5\text{-}C_5H_5)_2H_2] \geqslant 10:1$. The dependence on the concentration of acid was determined, in each case, from a graph of the observed rate constant (k_{obs}) against the concentration of HCl (Figs. 3, 10 and 12).

NMR Spectroscopy Experiments.—All NMR spectroscopy experiments (^1H, ^2H, ^{13}C, low-temperature and relaxation) were recorded on a JEOL GSX 270 spectrometer. ^1H, ^2H and ^{13}C NMR spectra were all referenced against $SiMe_4$.

Relaxation Rates of Hydrides in $[W(\eta^5\text{-}C_5H_5)_2H_3]^+$.—The relaxation rates of the hydrides associated with $[W(\eta^5\text{-}C_5H_5)_2H_3]^+$ were measured at 25.0 °C in CF_3CO_2H (Aldrich) by the usual 180°–τ–90° pulse sequence, with τ = 10–4000 ms (Fig. 6). The relaxation rate constants were determined from graphs of $\log_e(I_\tau - I_\infty)$ against τ, where I_τ is the measured intensity of the hydride signal at pulse interval τ. The value of I_∞ was determined at 25 000 ms.

Monitoring the Reaction Between $[Mo(\eta^5\text{-}C_5H_5)_2H_2]$ *and* HCl. The reaction between $[Mo(\eta^5\text{-}C_5H_5)_2H_2]$ and HCl was followed on the NMR spectrometer at low temperature in the following manner. A known volume of a solution of the dihydride (concentration = 40 mmol dm^{-3}) in $[^2H_8]$thf (1.0 cm^3) was frozen at −196 °C in a 10 mm NMR tube. A known volume of stock HCl (prepared from equimolar amounts of $SiMe_3Cl$ and MeOH) in $[^2H_8]$thf was added to the tube so that the acid froze above the frozen complex solution. The volume of acid added was such that, when thawed, the concentration of HCl in the whole solution was known. The frozen solution was quickly transferred into the probe of the spectrometer which had been pre-cooled to −100 °C. Spectra were then recorded at regular intervals until the reaction was complete (Fig. 11). Monitoring the reaction at −100 °C has the advantage that, although the solvent and HCl are liquids, and the $[Mo(\eta^5\text{-}C_5H_5)_2H_2]$ is in solution at this temperature, the $SiMe_3(OMe)$ side-product (from the formation of anhydrous HCl in thf) is not. Signals attributable to this material [δ 0.4 (s, 9 H, $SiMe_3$), 3.4 (s, 3 H, OMe)] are observed only when the temperature is raised above −60 °C.

IR spectra were recorded on a Perkin Elmer 883 spectrometer as KBr discs.

Results and Discussion

Mechanistically, the protonation of hydrido complexes to form a dihydride can occur by two distinct pathways: either direct protonation of the metal, or protonation of a hydrido ligand to give an intermediate dihydrogen species, which then undergoes an intramolecular oxidative-cleavage to give the dihydride, as shown in Fig. 1. In principle it is possible to distinguish between these two pathways by the detection of the intermediate dihydrogen species.

One of the simplest protonation reactions is that of $[M(\eta^5\text{-}C_5H_5)_2H_2]$ (M = Mo or W)[11] shown in equation (2). Recently, product analyses[12,13] of the deuteriation reactions of the analogous $[W(\eta^5\text{-}C_5Me_5)_2H_2]$ have indicated that the initial site of attack is a hydrido ligand. The proposed dihydrogen species $[W(\eta^5\text{-}C_5Me_5)_2H(\eta^2\text{-}H_2)]^+$ subsequently forms the trihydride product. We now report kinetic and mechanistic studies on $[M(\eta^5\text{-}C_5H_5)_2H_2]$ which confirm this proposal, at least for M = W, and demonstrate that for M = Mo the reaction is more complicated and involves an intermediate binuclear species.

Reaction of $[W(\eta^5\text{-}C_5H_5)_2H_2]$ *with* HCl.—When studied with a stopped-flow spectrophotometer the reaction between $[W(\eta^5\text{-}C_5H_5)_2H_2]$ and an excess of anhydrous HCl in thf shows spectroscopic behaviour characteristic of the formation of a spectrophotometrically detectible intermediate which subsequently collapses to form an equilibrium concentration of product, Fig. 2.

Thus upon mixing the two reactants there is an initial, rapid absorbance decrease, which is complete within the dead-time of the stopped-flow apparatus (2.0 ms), followed by an exponential absorbance–time curve to yield the product. The magnitude of the initial absorbance decrease depends on the concentration of HCl, such that at low acid concentrations the absorbance change is small (and the subsequent exponential trace is an absorbance decrease), whereas at high acid concentrations the absorbance change is sufficiently large that the following exponential trace is an absorbance increase. The final absorbance also depends on the concentration of HCl demonstrating the equilibrium nature of this reaction.

The kinetics associated with the absorbance–time curve exhibit a simple first-order dependence on the concentration of complex as demonstrated by the exponential nature of these curves and the independence of k_{obs} (observed first-order rate constant) on the concentration of complex over the range,

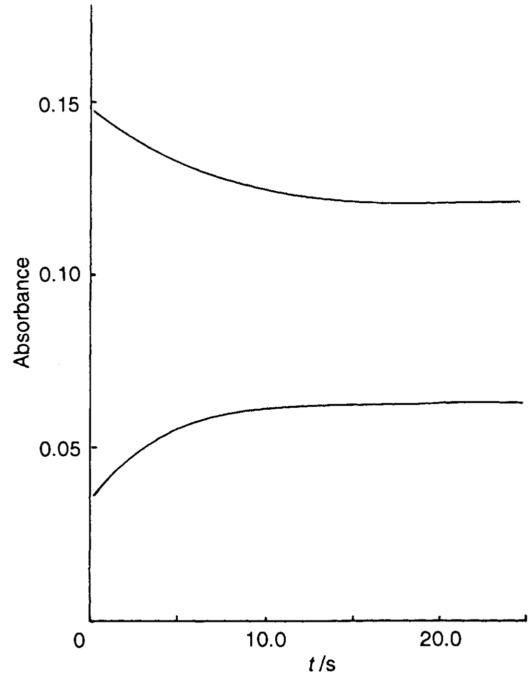

Fig. 2 Absorbance–time trace for the equilibrium reaction between $[W(\eta^5\text{-}C_5H_5)_2H_2]$ (0.25 mmol dm^{-3}) and anhydrous HCl in thf at 25.0 °C (I = 0.1 mol dm^{-3}, $[NBu^n{}_4]BF_4$). Top curve: [HCl] = 5.0 mmol dm^{-3}; bottom curve: [HCl] = 100.0 mmol dm^{-3}. In the absence of acid the absorbance of $[W(\eta^5\text{-}C_5H_5)_2H_2]$ is 0.25

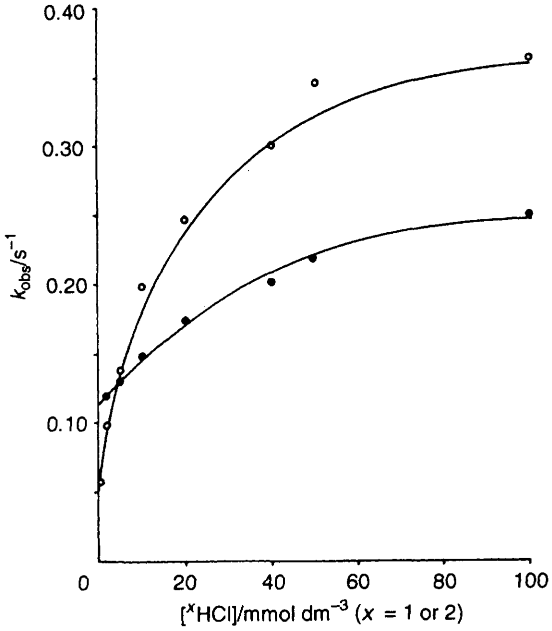

Fig. 3 Dependence of k_{obs} on the concentration of HCl for the equilibrium reaction with $[W(\eta^5-C_5H_5)_2H_2]$ in thf at 25 °C (I = 0.1 mol dm^{-3}, $[NBu^n_4]BF_4$). Data points correspond to HCl (●) and DCl (○). Curves drawn are those defined by equation (4), using the values given in the text

[W] = 0.5–0.05 mmol dm^{-3}. The dependence on the concentration of HCl is complicated as shown in Fig. 3.

At low concentrations of acid the rate of the reaction exhibits a first-order dependence on the concentration of HCl, but at high concentrations of acid the rate of the reaction becomes independent of the HCl concentration. The addition of chloride ions in the concentration range $[PBu^n_4]Cl$ = 0–10 mmol dm^{-3} has no effect on the rate of the reaction. The data can be fitted to equation (3). This rate law is consistent with the mechanism

$$k_{obs} = (0.11 \pm 0.01) + \frac{(56 \pm 3)\,[HCl]}{1 + (40 \pm 3)\,[HCl]} \qquad (3)$$

shown in Scheme 1, involving coupled equilibria.

Within the dead-time of the stopped-flow apparatus there is a rapid protonation of the complex to generate an intermediate dihydrogen complex which subsequently (over the next few seconds) equilibrates with the classical hydride tautomer. There are several aspects of this scheme which require further elaboration; in particular concerning the identity of the initial protonation species. There are three positions where this initial protonation can occur: the metal, a hydrido ligand or a cyclopentadienyl ring.[14] Clearly this rapid protonation does not occur at the metal since this would result in the direct formation of the product, $[W(\eta^5-C_5H_5)_2H_3]^+$. In order to distinguish between the remaining possibilities (hydride or cyclopentadienyl ring) we have isolated the products from the reaction between $[W(\eta^5-C_5H_5)_2H_2]$ and an excess of DCl in thf, $[W(\eta^5-C_5H_5)_2D_3]DCl_2$. Both ^2H NMR and IR spectroscopy show that deuterium is incorporated only into the hydrides [NMR: δ −6.8, W–D), IR ν(W–D) 1200 cm^{-1}] and none into the cyclopentadienyl rings. In addition, there is no incorporation of deuterium into the cyclopentadienyl rings even in neat CF_3CO_2D over at least 3 h. Clearly these results mitigate against proton attack at the cyclopentadienyl residues.

The rate law associated with the mechanism in Scheme 1 is given by equation (4).[15]

$$k_{obs} = k_{-3} + \frac{k_3 K_1 [HCl]}{1 + K_1 [HCl]} \qquad (4)$$

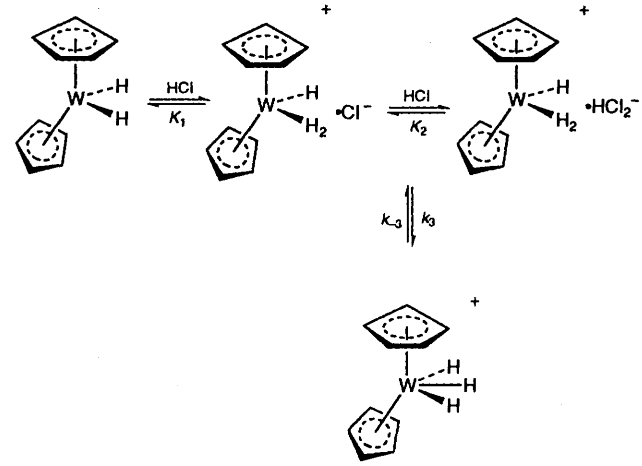

Scheme 1

By comparison of equations (3) and (4) the values k_{-3} = 0.11 ± 0.01 s^{-1}, k_3 = 0.14 ± 0.01 s^{-1} and K_1 = 40 ± 3 dm^3 mol^{-1} can be determined. The same form of rate law was observed for the very similar protonation reaction of $[WH_4(PMePh_2)_4]$, also involving a dihydrogen complex intermediate.[8]

Further detail about this mechanism is obtainable from analysis of the magnitude of the initial absorbance change and its dependence on the concentration of HCl. This analysis is shown in Fig. 4.

The interesting feature of this spectrophotometric analysis is that the derived equilibrium constant, K_0, is given equation (5).

$$K_0 = K_1K_2 = \frac{[W(\eta^5-C_5H_5)_2H(\eta^2-H_2)^+\cdot HCl_2^-]_e}{[W(\eta^5-C_5H_5)_2H_2]_e[HCl]^2} \qquad (5)$$

The second-order dependence on the concentration of HCl in equation (5) stands in stark contrast to the first-order dependence on the concentration of acid established in the kinetic analysis. However, these two results are not incompatible. Indeed the spectrophotometric analysis indicates that there are two identically reactive protonation species in solution $\{[W(\eta^5-C_5H_5)_2H(\eta^2-H_2)]^+X^-$, X = Cl or $HCl_2\}$, which differ only in the nature of the anion to which the cation is ion-paired in this low dielectric constant solvent thf. Since K_1 = 40 cm^3 mol^{-1} (from the kinetic analysis), we can derive K_2 = (6.6 ± 0.4) × 10^2 dm^3 mol^{-1}. A similar analysis of the data with DCl (see below) gives K_1^D = 70 dm^3 mol^{-1} (from the kinetics) and K_2^D = (6.8 ± 0.3) × 10^2 dm^3 mol^{-1}. The agreement in the two derived values of K_2 and K_2^D demonstrates the internal consistency of this analysis. Clearly the kinetics will only reflect the value of K_1 since this is the constant which defines the concentration of $[W(\eta^5-C_5H_5)_2H(\eta^2-H_2)]^+$; the constant K_2 merely partitions the species between the two equally reactive ion-pairs $[W(\eta^5-C_5H_5)_2H(\eta^2-H_2)]^+\cdot X^-$. The simplicity of the mechanism shown in Scheme 1 permits us to discuss some of the fundamental kinetic and thermodynamic aspects of dihydrogen complexes.

Acidity of Dihydrogen Complexes.—It has been proposed that dihydrogen complexes are more acidic than the 'classical' dihydride[3,7,16] analogues. However, it is only with this study that this effect can be fully and rigorously quantified. The acid strength of $[W(\eta^5-C_5H_5)_2H(\eta^2-H_2)]^+$ is measured directly from the value K_1 = 40 cm^3 mol^{-1}. Of course this value relates to the acidity in thf. The acid strength of the corresponding 'classical' hydride, $K_1{}^1$, is given by the expression in equation (6).

$$K_1{}^1 = K_1K_3 = \frac{[W(\eta^5-C_5H_5)_2H_3{}^+]_e}{[W(\eta^5-C_5H_5)_2H_2]_e[HCl]} \qquad (6)$$

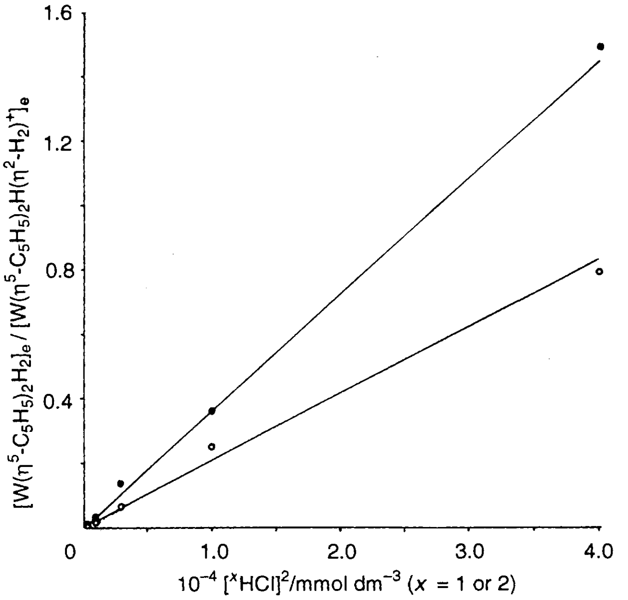

Fig. 4 Determination of the protonation equilibrium constant, K_0, for $[W(\eta^5\text{-}C_5H_5)_2H_2]$ with anhydrous HCl in thf at 25 °C ($I = 0.1$ mol dm^{-3}, $[NBu^n_4]BF_4$) calculated from the initial absorbance change (see text). The equilibrium concentrations $[W(\eta^5\text{-}C_5H_5)_2H_2]_e$ and $[W(\eta^5\text{-}C_5H_5)_2H(\eta^2\text{-}H_2)^+\cdot X^-]_e$ (X = Cl or HCl_2) were calculated from the measured initial absorbance using the molar absorption coefficients: $\varepsilon_{WH} = 1.0 \times 10^3$ and $\varepsilon_{WH_2} = 1.4 \times 10^2$ dm^3 mol^{-1} cm^{-1} for these two species at λ = 350 nm respectively. Data points correspond to HCl (●) and DCl (○). The observed equilibrium constants correspond to $K_0 = K_1K_2 = [W(\eta^5\text{-}C_5H_5)_2H(\eta^2\text{-}H_2)^+\cdot X^-]_e/[W(\eta^5\text{-}C_5H_5)_2H_2]_e[HCl]^2$

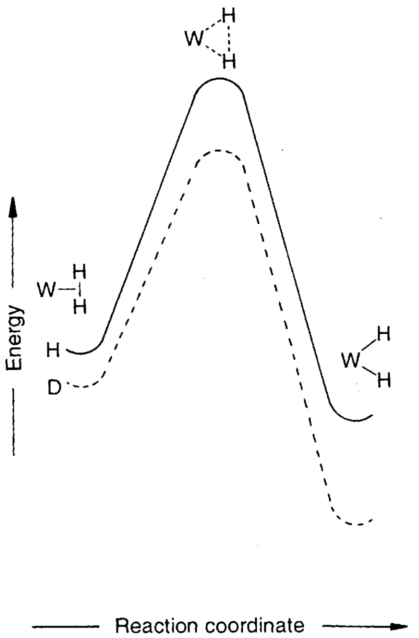

Fig. 5 Reaction coordinate profile for the equilibrium between $[W(\eta^5\text{-}C_5H_5)_2H(\eta^2\text{-}H_2)]^+$ and $[W(\eta^5\text{-}C_5H_5)_2H_3]^+$ in thf at 25.0 °C, showing the relative zero-point energies for the reactions with HCl and DCl

From the established values of K_1 and K_3 we can calculate $K_1{}^1 = (52 \pm 5)$ dm^3 mol^{-1}. Hence, for this system, there is little difference in the acid strengths of the dihydrogen and 'classical' hydride forms. In general, the ratio of acid strengths for the two tautomers is given by K_3. A survey of the literature shows that the measured values of K_3, in a variety of complexes, cover the range $K_2 = 0.5$–3.9.[8,17–20] However, in general there is no restriction on the value of K_3 and hence there can be no general criterion concerning the acid strengths of the hydride and dihydrogen tautomers.

Protonation Pathways and Isotope Effects.—Of course the rate law and the associated mechanism dictates that the *exclusive pathway* for proton transfer in this system is *via* the dihydrogen ligand. Clearly, direct protonation or deprotonation of the metal is a much slower process than at the hydride ligand.

The influence of DCl on the reaction with $[W(\eta^5\text{-}C_5H_5)_2H_2]$ is shown in Fig. 3. Analysis of these data in terms of equation (4) gives: $(K_1{}^H/K_1{}^D) = 0.39 \pm 0.05$, $(k_3{}^H/k_3{}^D) = 0.43 \pm 0.05$, $(k_{-3}{}^H/k_{-3}{}^D) = 2.20 \pm 0.01$, and hence $(K_3{}^H/K_3{}^D) = 0.20 \pm 0.05$. The kinetic isotope effects associated with k_3 and k_{-3} gives information about the relative zero-point energies of the hydride and dihydrogen species. As illustrated in Fig. 5 both $[W(\eta^5\text{-}C_5H_5)_2H(\eta^2\text{-}H_2)]^+$ and $[W(\eta^5\text{-}C_5H_5)_2H_3]^+$ must interconvert *via* the same transition state, in which the dihydrogen residue has an elongated H–H bond.

Since $(k_3{}^H/k_3{}^D) = 0.43$ it is clear that the difference in zero-point energies of the transition state must be larger than that for the dihydrogen complex. In addition, since $(k_{-3}{}^H/k_{-3}{}^D) = 2.20$ it follows that the difference in zero-point energies for $[W(\eta^5\text{-}C_5H_5)_2H_3]^+$ is larger again. Thus the zero-point energy differences in this system increase as the intramolecular hydrogen–hydrogen distances increases. However, it seems unlikely that this pattern is general. There are few quantitative studies with which to compare our results, but studies on the equilibrium shown in equation (7)[19] demonstrate that $K_3{}^H/K_3{}^D = 1.3$ at 25.0 °C (using the notation employed in this paper); a very different effect to that observed for $[W(\eta^5\text{-}C_5H_5)_2H_2]$.

$$[Nb(\eta^5\text{-}C_5H_5)(CO)_3(\eta^2\text{-}H_2)] \overset{K_3}{\rightleftharpoons} [Nb(\eta^5\text{-}C_5H_5)(CO)_3H_2] \quad (7)$$

The only other study where isotope effects have been determined is for the reaction shown in equation (8), where $(k_{-3}{}^H/k_{-3}{}^D) = 1.08$.

$$[W(CO)_3\{P(C_6H_{11})_3\}_2H_2] \underset{k_3}{\overset{k_{-3}}{\rightleftharpoons}} [W(CO)_3\{P(C_6H_{11})_3\}_2(\eta^2\text{-}H_2)] \quad (8)$$

The kinetics do not allow a determination of the value, $(k_3{}^H/k_3{}^D)$ in this system. Looking at the results from our study together with these other two, it seems unlikely that isotope effects on the tautomerisation reactions can be used as a diagnostic test for characterising transient dihydrogen species. Clearly there is a need to establish a diagnostic kinetic parameter for dihydrogen species which are intermediates, since the criteria established so far are of limited applicability to reactive intermediates. For instance, ^1H NMR and IR spectroscopy is of limited applicability, not only because of the short lifetime of reactive dihydrogen intermediates, but also because they are often in rapid equilibrium with the 'classical' form and the parent hydride (by proton exchange), resulting in an average signal.

Characterisation of the Reaction Product.—The product mixture from the reaction between $[W(\eta^5\text{-}C_5H_5)_2H_2]$ and HCl consists of the parent hydride together with $[W(\eta^5\text{-}C_5H_5)_2H(\eta^2\text{-}H_2)]^+$ and $[W(\eta^5\text{-}C_5H_5)_2H_3]^+$. At high concentrations of acid the product is predominantly the two cationic tautomers, but the value of $K_3 = 1.4$ means that, even under these conditions, there is always 42% $[W(\eta^5\text{-}C_5H_5)_2H(\eta^2\text{-}H_2)]^+$ present. Consequently the ^1H NMR spectrum of the reaction product in thf shows only an average signal (δ −6.8, s, W–H). In principle it is possible to identify this mixture as containing a dihydrogen species from the characteristic short relaxation time ($T_1 < 80$ ms)[3,22,23] of the dihydrogen complexes.

In an equilibrium mixture of $[W(\eta^5\text{-}C_5H_5)_2H(\eta^2\text{-}H_2)]^+$ and $[W(\eta^5\text{-}C_5H_5)_2H_3]^+$ the observed relaxation time of the hydride signal (T_{obs}) will correspond to the proportions of each tautomer, as described by equation (9).

$$T_{obs} = T_{W\text{-}H_2}[W\text{-}H_2]_e + T_{W\text{-}H}\left[W\begin{smallmatrix}\diagup H\\ \diagdown H\end{smallmatrix}\right]_e \qquad (9)$$

A short value for T_{obs} will only be observed if: (*i*) there is an appreciable amount of the dihydrogen species present and, (*ii*) if the relaxation time of the 'classical' tautomer is not so long as to dominate T_{obs} completely. The limitations imposed by this second point are particularly well illustrated in the $[W(\eta^5\text{-}C_5H_5)_2H_2]$ system.

We have measured the relaxation times of the hydrides in $[W(\eta^5\text{-}C_5H_5)_2H_3]^+$ in CF_3CO_2H at 25.0 °C. This solvent was chosen to avoid complications associated with proton dissociation from the trihydride. The observed spectra are shown in Fig. 6. The A_2X pattern is consistent with the planar geometry of the three hydride ligands, as noted before.[11,12] The signal associated with the central hydride H_c [δ −6.50 (t, 1 H, $^2J_{HH}$ 9.4, $^1J_{WH_c}$ 34.5 Hz) has a relaxation time T_c = 1.70 s (at 270 MHz), and the signal associated with the two peripheral hydrides H_p [δ −7.08 (d, 2 H, $^2J_{HH}$ 9.42, $^1J_{WH_p}$ 22.9 Hz) has a relaxation time T_p = 2.9 s (at 270 MHz). These are very long relaxation times and it is clear that their contribution to equation (9) means that they will dominate T_{obs}, and effectively mask any contribution from $[W(\eta^5\text{-}C_5H_5)_2H(\eta^2\text{-}H_2)]^+$. Thus even this criterion for establishing the existence of dihydrogen species is of limited value in systems which are equilibrium mixtures.

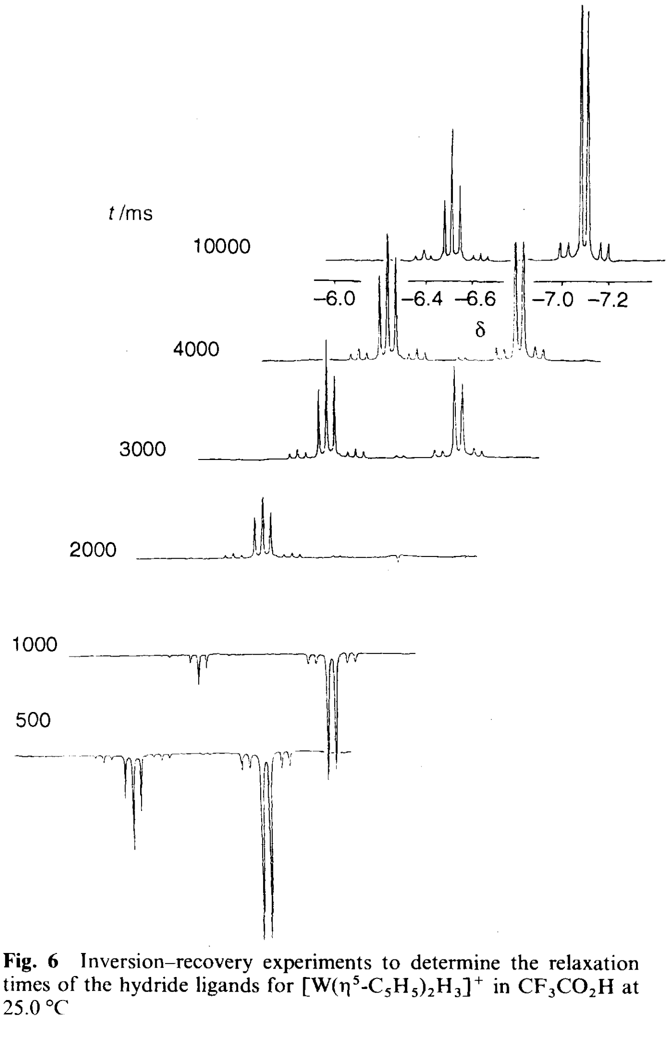

Fig. 6 Inversion–recovery experiments to determine the relaxation times of the hydride ligands for $[W(\eta^5\text{-}C_5H_5)_2H_3]^+$ in CF_3CO_2H at 25.0 °C

Reaction of $[Mo(\eta^5\text{-}C_5H_5)_2H_2]$ *with* HCl.—It might reasonably be expected that the mechanism of the reaction between $[Mo(\eta^5\text{-}C_5H_5)_2H_2]$ and HCl is essentially the same as that defined for the tungsten analogue. However, kinetic and spectroscopic analysis of the protonation of the molybdenum complex shows important differences from that of the tungsten analogue.

When studied with a stopped-flow spectrophotometer the reaction between $[Mo(\eta^5\text{-}C_5H_5)_2H_2]$ and an excess of anhydrous HCl in thf exhibits a biphasic absorbance–time trace, typified by that shown in Fig. 7.

The two phases which comprise the formation of $[Mo(\eta^5\text{-}C_5H_5)_2H_3]^+$ are first, an initial rapid increase in absorbance to form an intermediate, followed by an absorbance decay to give the product. Both of these stages in the reaction will be discussed separately. However, before we proceed with this discussion it is important to appreciate that in this system the absorbance of the intermediate and the final product are independent of the concentration of acid. These observations demonstrate that under our conditions the protonation of $[Mo(\eta^2\text{-}C_5H_5)_2H_2]$ by HCl in thf is not an equilibrium reaction. This is in clear contrast to the established behaviour of the tungsten analogue under identical conditions.

Formation of the Intermediate Binuclear Species.—As we have seen in the reaction of $[W(\eta^5\text{-}C_5H_5)_2H_2]$ with HCl, the intermediate, $[W(\eta^5\text{-}C_5H_5)_2H(\eta^2\text{-}H_2)]^+$, is detectable. However, the visible absorption spectrum of the intermediate detected in the analogous molybdenum reaction is markedly different from that of the dihydrogen complex, as shown in Fig. 8.

Although both spectra are essentially featureless, the spectrum of $[W(\eta^5\text{-}C_5H_5)_2H(\eta^2\text{-}H_2)]^+$ is what one would intuitively expect for this species: an absorbance very similar to that of the tautomer $[W(\eta^5\text{-}C_5H_5)_2H_3]^+$ at all wavelengths, provided that no significant geometrical changes occur upon protonation. Indeed, a similar spectral behaviour has been observed[8] for $[WH_3(\eta^2\text{-}H_2)(PMePh_2)_4]^+$ and $[WH_5(PMePh_2)_4]^+$. In contrast, the spectrum of the intermediate observed in the reaction with $[Mo(\eta^5\text{-}C_5H_5)_2H_2]$ is much more

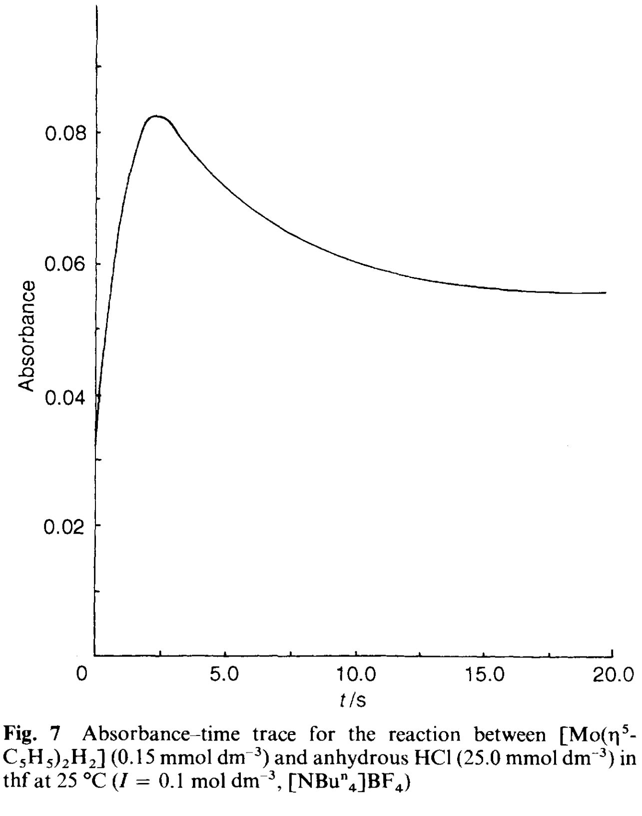

Fig. 7 Absorbance–time trace for the reaction between $[Mo(\eta^5\text{-}C_5H_5)_2H_2]$ (0.15 mmol dm^{-3}) and anhydrous HCl (25.0 mmol dm^{-3}) in thf at 25 °C (I = 0.1 mol dm^{-3}, $[NBu^n{}_4]BF_4$)

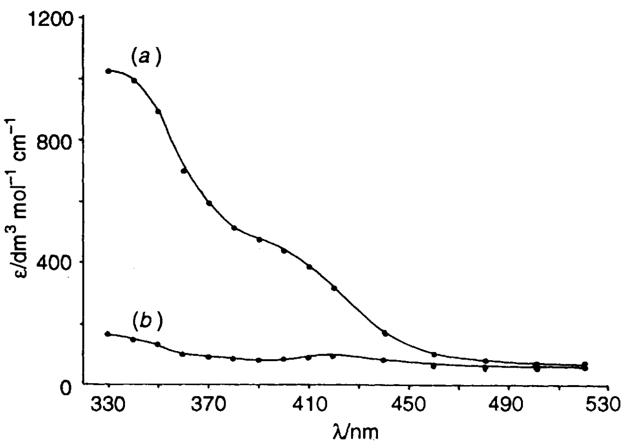

Fig. 8 Visible absorption spectra of the intermediates detected in the reactions between $[Mo(\eta^5\text{-}C_5H_5)_2H_2]$ (*a*) or $[W(\eta^5\text{-}C_5H_5)_2H_2]$ (*b*) with anhydrous HCl in thf, [HCl] = 100 mmol dm^{-3}. Molar absorption coefficients correspond to molar concentrations of Mo or W respectively

intense than that of $[W(\eta^5\text{-}C_5H_5)_2H(\eta^2\text{-}H_2)]^+$, and it seems unlikely that this represents the spectrum of $[Mo(\eta^5\text{-}C_5H_5)_2H(\eta^2\text{-}H_2)]^+$. It is also unlikely that the intermediate detected in the molybdenum system is that of $[Mo(\eta^5\text{-}C_5H_5)(\eta^4\text{-}C_5H_6)H_2]^+$, formed by proton attack at the cyclopentadienyl ring, since both ^2H NMR and IR spectra of the product formed in the reaction between $[Mo(\eta^5\text{-}C_5H_5)_2H_2]$ and DCl in thf shows no incorporation of deuterium into the cyclopentadienyl rings, only into the hydride ligands [NMR, δ −0.1 (s, Mo–D); IR, ν(Mo–D) 1100 cm^{-1}]. Parenthetically, we note that in thf the hydride signal in the NMR spectrum of $[Mo(\eta^5\text{-}C_5H_5)_2H_3]^+$ is at low field compared to that observed in CF_3CO_2H (δ −6.6, s). This shift is a direct consequence of the change in solvent since an isolated sample of $[Mo(\eta^5\text{-}C_5H_5)_2H_3]Cl$ exhibits the hydride signal δ −6.6 in CF_3CO_2H and C_6D_6, but δ −0.1 in $[^2H_8]$thf. This shift may, in part, be attributable to ion-pairing in thf, where a chloride ion specifically interacts with the hydride ligands. Certainly the ^1H NMR spectrum of the neutral $[Mo(\eta^5\text{-}C_5H_5)_2H_2]$ has hydride signals at δ −8.8 in both C_6D_6 and $[^2H_8]$thf.

We propose that the spectroscopically detected intermediate in the reaction with $[Mo(\eta^5\text{-}C_5H_5)_2H_2]$ is a binuclear species and this conclusion is consistent with the kinetics for the formation of this intermediate. The biphasic absorbance–time behaviour, typified by that shown in Fig. 7, can be satisfactorily fitted to exponential curves. However, there are two reasons why we believe that the initial phase should not be analysed in this manner. First, it is only possible to monitor *ca.* 70% of the initial phase before the second phase distorts the shape. Monitoring only 70% of the absorbance trace is insufficient to ensure that the curve is a true exponential. In particular a reaction which is second-order in the molybdenum complex would be essentially indistinguishable from that exhibiting a first-order dependence on the complex concentration over this reaction period.[24] Secondly, when analysed for a first-order dependence on the concentration of $[Mo(\eta^5\text{-}C_5H_5)_2H_2]$, the derived values of k_{obs} vary with the concentration of complex: a behaviour inconsistent with a simple first-order dependence on the concentration of $[Mo(\eta^5\text{-}C_5H_5)_2H_2]$.

Analysis of the data for the formation of the intermediate in terms of a second-order dependence on the concentration of $[Mo(\eta^5\text{-}C_5H_5)_2H_2]$,[24] as shown in Fig. 9, gives a more consistent behaviour. Thus graphs of $[Mo]_t^{-1} - [Mo]_\infty^{-1}$ *versus t* are straight lines and the derived values of k^1_{obs} (pseudo second-order rate constant) are independent of the complex concentration.

The value k^1_{obs} exhibits a linear dependence on the concentration of HCl, as shown in Fig. 10, and the complete rate

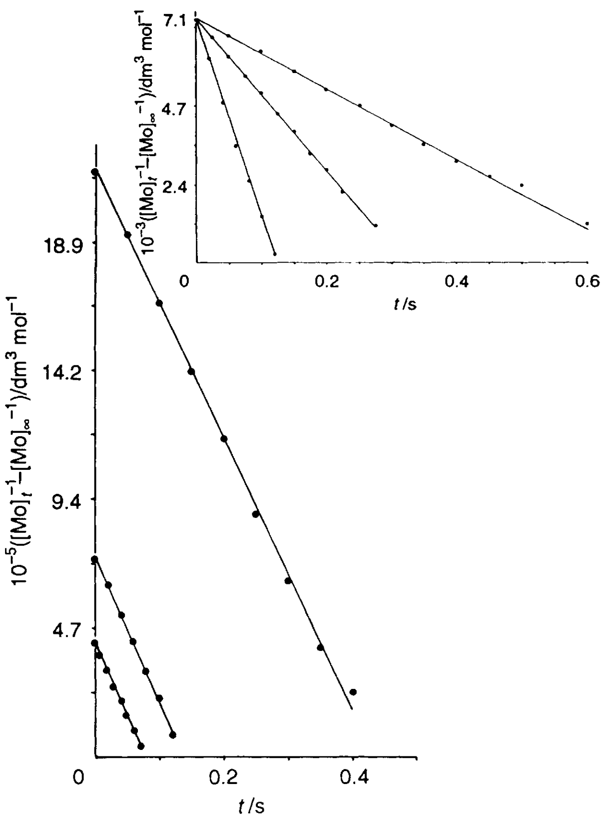

Fig. 9 Plot of $\{[Mo(\eta^5\text{-}C_5H_5)_2H_2]_t^{-1} - [Mo(\eta^5\text{-}C_5H_5)_2H_2]_\infty^{-1}\}$ *versus t* for the initial phase of the reaction between $[Mo(\eta^5\text{-}C_5H_5)_2H_2]$ and anhydrous HCl in thf at 25 °C (I = 0.1 mol dm^{-3}, $[NBu^n{}_4]BF_4$). The insert shows the influence of acid concentration, $[Mo(\eta^5\text{-}C_5H_5)_2H_2]$ = 0.15, [HCl] = 5.0–40.0 mmol dm^{-3}. Main picture shows the influence of varying the complex concentration, $[Mo(\eta^5\text{-}C_5H_5)_2H_2]$ = 0.25, 0.15 and 0.05 mmol dm^{-3}, [HCl] = 40.0 mmol dm^{-3}

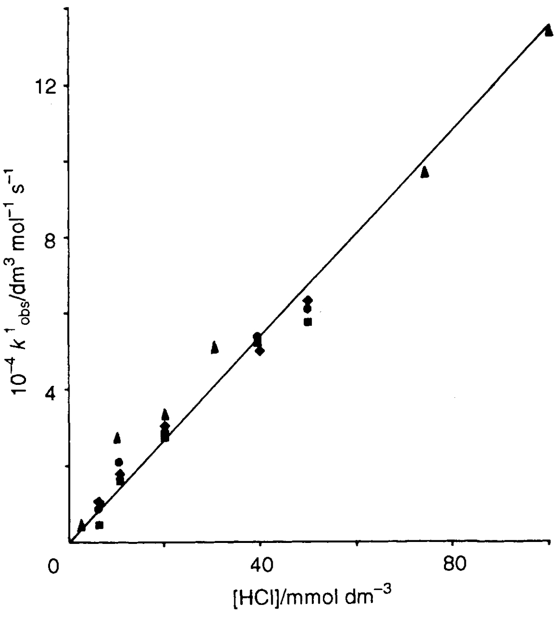

Fig. 10 Dependence of k^1_{obs} (pseudo-second-order rate constant) on the concentration of HCl for the initial phase of the reaction between $[Mo(\eta^5\text{-}C_5H_5)_2H_2]$ and anhydrous HCl in thf at 25 °C (I = 0.1 mol dm^{-3}, $[NBu^n{}_4]BF_4$). Data points correspond to $[Mo(\eta^5\text{-}C_5H_5)_2H_2]$ = 0.5 (●), 0.25 (▲), 0.15 (■) and 0.05 mmol dm^{-3} (◆). Line drawn is that defined by equation (10)

law for the formation of the intermediate is given by equation (10).

$$\frac{-\mathrm{d}[\mathrm{Mo}(\eta^5\text{-}C_5H_5)_2H_2]}{\mathrm{d}t} = (1.35 \pm 0.1) \times 10^6[\mathrm{HCl}][\mathrm{Mo}(\eta^5\text{-}C_5H_5)_2H_2]^2 \quad (10)$$

Although the second-order dependence on the concentration of $[\mathrm{Mo}(\eta^5\text{-}C_5H_5)_2H_2]$ can be indicative of the formation of a binuclear species, this kinetic analysis can clearly give no information concerning the structure of this binuclear, nor indeed the order of the elementary reactions by which it is formed. It seems unlikely that the binuclear species is formed by an initial dimerisation of $[\mathrm{Mo}(\eta^5\text{-}C_5H_5)_2H_2]$ since there is no evidence for such a process from other studies on this complex. Indeed the ^{1}H and ^{13}C NMR spectra of $[\mathrm{M}(\eta^5\text{-}C_5H_5)_2H_2]$ are essentially identical for Mo and W analogues [NMR (C_6D_6): ^{1}H, δ 4.36 (s, 5 H, C_5H_5) and −8.8 (s, 1 H, Mo–H); ^{13}C, δ 75.6 (d of qnt, $^1J_{CH}$ 178.6, $^3J_{CH}$ 6.6 Hz)]. Rather, it seems more likely that the binuclear intermediate results from the pathway shown in Scheme 2.

Thus we propose that the initial protonation of $[\mathrm{Mo}(\eta^5\text{-}C_5H_5)_2H_2]$ occurs at a hydride ligand to give the dihydrogen species $[\mathrm{Mo}(\eta^5\text{-}C_5H_5)_2H(\eta^2\text{-}H_2)]^+$. This is identical to the initial step in the protonation of the tungsten analogue. However, whereas the reaction of $[\mathrm{W}(\eta^5\text{-}C_5H_5)_2H(\eta^2\text{-}H_2)]^+$ proceeds directly to form the product by intramolecular oxidative cleavage of the dihydrogen ligand, for the molybdenum system a more rapid reaction ensues in which the cationic dihydrogen species attacks the parent, $[\mathrm{Mo}(\eta^5\text{-}C_5H_5)_2H_2]$.

In order to obtain structural information about this binuclear intermediate, which is so short-lived (τ = 20 s) at 25.0 °C, we performed the reaction in the probe of an NMR spectrometer at −100 °C with $[\mathrm{HCl}]:[\mathrm{Mo}(\eta^5\text{-}C_5H_5)_2H_2] = 2\text{–}5:1$. Under these conditions the reaction is sufficiently slow that it can be followed over the course of a couple of hours. The spectral changes observed are shown in Fig. 11.

There are three important points to be made about these data. (1) Under the conditions of these experiments we can detect a resonance attributable to an intermediate (δ 3.1, probably MoH of the binuclear species). This intermediate is formed before any product is detected, and dies away as the product accumulates. It is worth noting that other binuclear hydrido and dihydrogen species can show only a single hydride resonance in the ^{1}H NMR spectrum, because of rapid intramolecular exchange.[25,26] (2) There are only minor changes in the cyclopentadienyl region (δ 4.5) of the spectra, associated with the minor shift in peak position of reactant and product. That there is no more complex set of signals formed during the lifetime of the intermediate militates against a binuclear species involving coupling of the cyclopentadienyl rings, and indicates that the intermediate presumably has bridging hydrido group(s) as shown in Scheme 2. (3) The peak attributable to the hydrides in $[\mathrm{Mo}(\eta^5\text{-}C_5H_5)_2H_2]$ (δ −9.6) is observed throughout the reaction. From the spectra in Fig. 11 it seems that the concentration of $[\mathrm{Mo}(\eta^5\text{-}C_5H_5)_2H_2]$ roughly keeps apace of the dimer concentration.

We must emphasise that the structures we have proposed for the binuclear intermediates in Scheme 2 are only tentative. However, our proposed structure for $[\{\mathrm{Mo}(\eta^5\text{-}C_5H_5)_2H_2\}_2(\mu\text{-}H)]^+$ is based on that of the crystallographically established[27] $[\{\mathrm{W}(\eta^5\text{-}C_5H_5)_2H\}_2(\mu\text{-}H)]^+$. In addition, $[\mathrm{Mo}(\eta^5\text{-}C_5H_5)_2H_2]$

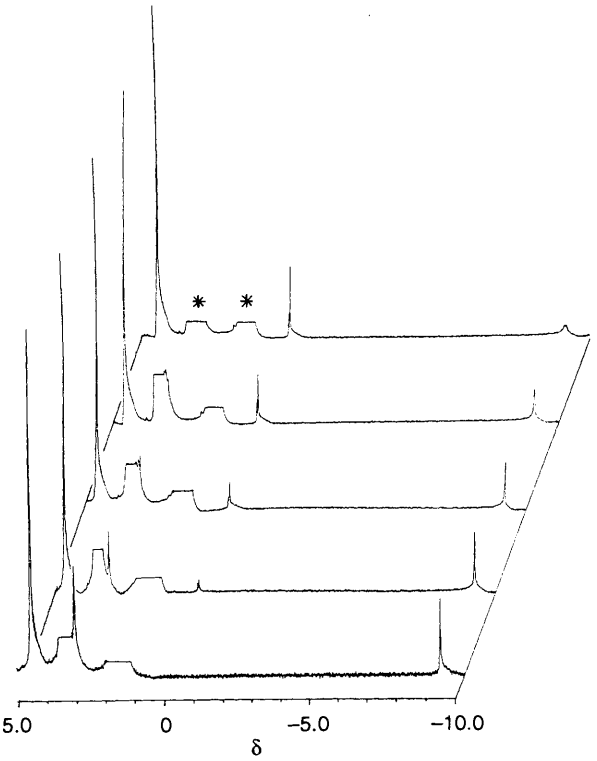

Fig. 11 Proton NMR spectral changes observed in the reaction between $[\mathrm{Mo}(\eta^5\text{-}C_5H_5)_2H_2]$ (40.0 mmol dm^{-3}) and anhydrous HCl (200.0 mmol dm^{-3}) in [$^2H_8$]thf at −100 °C. For clarity the peaks at δ 1.7 and δ 3.6 (marked with an asterisk), assignable to incompletely deuteriated thf, have been omitted. Spectra were recorded over a period of 2 h at *ca.* 35 min intervals

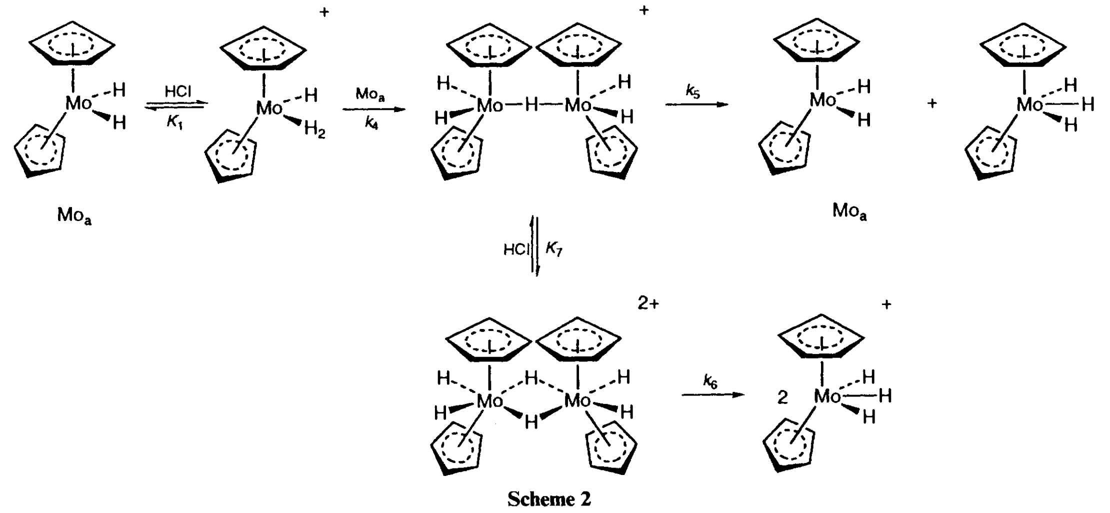

Scheme 2

is known to form complexes with other metals by using bridging hydride ligands.[28] Attempts to study the reaction of $[W(\eta^5\text{-}C_5H_5)_2H_2]$ with HCl by the same NMR method are thwarted by the insolubility of $[W(\eta^5\text{-}C_5H_5)_2H_3]HCl_2$.

From a consideration of Scheme 2, the kinetics for the formation of the binuclear species is given equation (11), assuming that the protonation of $[Mo(\eta^5\text{-}C_5H_5)_2H_2]$ is a rapidly established equilibrium.

$$\frac{-d[Mo(\eta^5\text{-}C_5H_5)_2H_2]}{dt} = \frac{K_1k_4[HCl][Mo(\eta^5\text{-}C_5H_5)_2H_2]^2}{(1 + K_1[HCl])^2} \quad (11)$$

If the protonation constant K_1 is small, and $K_1[HCl] \ll 1$, then the observed rate law is that shown in equation (12), in good agreement with that observed experimentally, equation (10).

$$\frac{-d[Mo(\eta^5\text{-}C_5H_5)_2H_2]}{dt} = K_1k_4[HCl][Mo(\eta^5\text{-}C_5H_5)_2H_2]^2 \quad (12)$$

Comparison of equations (10) and (12) gives the values $K_1k_4 = (1.35 \pm 0.1) \times 10^6$ dm^6 mol^{-2} s^{-1}, and hence $k_4 \geqslant (1.35 \pm 0.1) \times 10^6$ dm^3 mol^{-1} s^{-1} and $K_1 \leqslant 1$ dm^3 mol^{-1}. In the derivation of equation (11) we have assumed that the binuclear intermediate results from rapid scavenging of $[Mo(\eta^5\text{-}C_5H_5)_2H(\eta^2\text{-}H_2)]^+$ by the large excess of $[Mo(\eta^5\text{-}C_5H_5)_2H_2]$. This seems a reasonable hypothesis based on: (*i*) the charges of the two interacting species, and (*ii*) the small value of K_1 (much smaller than that observed with $[W(\eta^5\text{-}C_5H_5)_2H_2]$), which means that only a small proportion of $[Mo(\eta^5\text{-}C_5H_5)_2H_2]$ is converted into $[Mo(\eta^5\text{-}C_5H_5)_2H(\eta^2\text{-}H_2)]^+$.

Formation of $[Mo(\eta^5\text{-}C_5H_5)_2H_3]^+$ *from the Binuclear Intermediate*.—The kinetics associated with the break-up of the binuclear intermediate exhibit a simple first-order dependence on the concentration of the intermediate, as shown by the excellent exponential traces (exponential for at least four half-lives) and the derived values of k_{obs} which are independent of the complex concentration, $[Mo(\eta^5\text{-}C_5H_5)_2H_2] = 0.5$–$0.05$ mmol dm^{-3}. The formation of $[Mo(\eta^5\text{-}C_5H_5)_2H_3]^+$ from the binuclear species exhibits a dependence on the concentration of HCl as shown in Fig. 12, and described by equation (13).

$$\frac{-d[Mo(\eta^5\text{-}C_5H_5)_2H_3{}^+]}{dt} = \{(8.3 \pm 0.5) \times 10^{-2} + (2.07 \pm 0.1)[HCl]\}[\{Mo(\eta^5\text{-}C_5H_5)_2H_2\}_2(\mu\text{-}H)^+] \quad (13)$$

This rate law is consistent with the mechanism shown in Scheme 2, involving rate-limiting break-up of the binuclear species. In addition, the acid-dependent pathway observed at high acid concentrations can be accredited to a rapid protonation of the binuclear intermediate prior to the cleavage step.

This mechanism is also consistent with the ^{1}H NMR spectral changes shown in Fig. 11. In the acid-independent route in Scheme 2 the dimer breaks up to release one molecule of product, $[Mo(\eta^5\text{-}C_5H_5)_2H_3]^+$, and one molecule of the starting complex, $[Mo(\eta^5\text{-}C_5H_5)_2H_2]$. This dihydride complex then recycles through the system until all the material is converted to product. Hence, under the conditions of the ^{1}H NMR spectral experiments (low acid concentrations and low temperatures) we observe the $[Mo(\eta^5\text{-}C_5H_5)_2H_2]$ maintaining a steady-state concentration, which is matching that of the intermediate, at least approximately. At higher acid concentrations, where the acid-dependent pathway dominates, two molecules of the product, $[Mo(\eta^5\text{-}C_5H_5)_2H_3]^+$, are released upon break-up of the binuclear intermediate, and hence under these conditions the steady-state concentration of $[Mo(\eta^5\text{-}C_5H_5)_2H_2]$ presumably would not be observed.

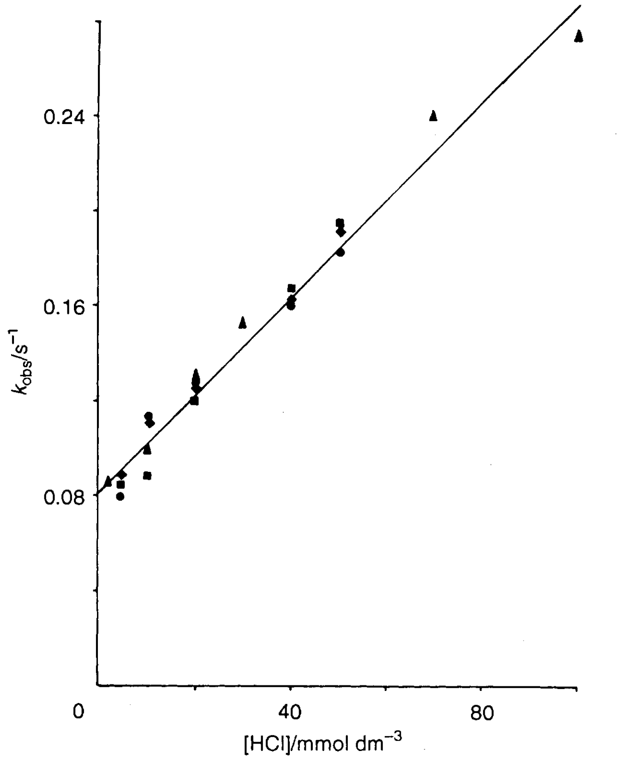

Fig. 12 Dependence of k_{obs} (pseudo-first-order rate constant) on the concentration of HCl for the second phase of the reaction between $[Mo(\eta^5\text{-}C_5H_5)_2H_2]$ and anhydrous acid in thf at 25 °C ($I = 0.1$ mol dm^{-3}, $[NBu^n{}_4]BF_4$). Data points correspond to $[Mo(\eta^5\text{-}C_5H_5)_2H_2] =$ 0.5 (●), 0.25 (▲), 0.15 (■) and 0.05 mmol dm^{-3} (◆). Line drawn is that defined by equation (13)

From Scheme 2, the kinetics of the decomposition of the binuclear intermediate is given by equation (14), where the protonation of the binuclear species is assumed to be a rapid pre-equilibrium prior to rate-limiting break-up of the dimer.

$$\frac{d[Mo(\eta^5\text{-}C_5H_5)_2H_3]^+}{dt} = \left\{\frac{k_5 + 2k_6K_7[HCl]}{1 + K_7[HCl]}\right\}[\{Mo(\eta^5\text{-}C_5H_5)_2H_2\}_2(\mu\text{-}H)^+] \quad (14)$$

If the protonation constant K_7 is small, and $K_7[HCl] \ll 1$, then equation (14) approximates to the rate law shown in equation (15) which is identical in form to the experimentally observed rate law shown in equation (13).

$$\frac{d[Mo(\eta^5\text{-}C_5H_5)_2H_3]^+}{dt} = \{k_5 + 2k_6K_7[HCl]\}[\{Mo(\eta^5\text{-}C_5H_5)_2H_2\}_2(\mu\text{-}H)^+] \quad (15)$$

Comparison of equations (13) and (15) permits the evaluation of $k_5 = (8.3 \pm 0.5) \times 10^{-2}$ s^{-1}, $k_6K_7 = (1.04 \pm 0.1)$ dm^3 mol^{-1} s^{-1}, with $K_7 \leqslant 1$ dm^3 mol^{-1} and $k_6 \geqslant (1.04 \pm 0.1)$ s^{-1}.

The protonation mechanisms of $[W(\eta^5\text{-}C_5H_5)_2H_2]$ and $[Mo(\eta^5\text{-}C_5H_5)_2H_2]$ shown in Schemes (1) and (2) respectively have the common features that the initial protonation is at a hydride ligand (and not the metal), and the product $[M(\eta^5\text{-}C_5H_5)_2H_3]^+$ is formed subsequently by an intramolecular oxidative cleavage of the dihydrogen ligand. However, in the

M = Mo case this simple reaction is complicated by the rapid formation of a binuclear species. The kinetics for the break-up of the binuclear species give us no information about the intimate details of the intramolecular cleavage step of the dihydrogen ligand. It should be emphasised that it is not entirely clear, at this stage, why the binuclear species should form in this protonation reaction. However, from the studies on $[W(\eta^5\text{-}C_5H_5)_2H_2]$ it is clear that the binuclear intermediate is not an essential precursor to dihydrogen cleavage. Rather that the binuclear is formed faster than the intramolecular oxidative-cleavage of $[Mo(\eta^5\text{-}C_5H_5)_2H(\eta^2\text{-}H_2)]^+$, and hence the dihydrogen species is enforced along the route involving the binuclear species. Nor do we know at what stage the oxidative-cleavage step occurs. It could either occur upon formation of the binuclear intermediate or it could be the step which triggers the cleavage of the binuclear species.

Conclusion

Understanding the sites and mechanisms of protonation of transition-metal hydride complexes is important not only in understanding the fundamental chemistry of these species, but also in defining the action of certain metalloenzymes at the atomic level. Most notably both the hydrogenases[29] and nitrogenases[1,30] have been proposed to involve hydrogen ligands as intermediates, formed by direct protonation of hydrido residues.

We have shown herein that the superficially simple protonation of $[M(\eta^5\text{-}C_5H_5)_2H_2]$ (M = Mo or W) to form $[M(\eta^5\text{-}C_5H_5)_2H_3]^+$ occurs by different pathways for the two analogues. In neither case does the proton bind directly to the metal; the proton preferentially attacks the hydride ligands. For the M = W case we are able to monitor the relatively simple intramolecular, oxidative-cleavage of the dihydrogen ligand. However, for M = Mo the rapid formation of a binuclear species hides the kinetic details of the oxidative-cleavage step, and complicates the kinetics of the initial protonation of $[M(\eta^5\text{-}C_5H_5)_2H_2]$.

This study, together with others which demonstrate direct protonation of hydride ligands,[4–8] poses the intriguing question whether this is always the mechanism for protonation of hydride complexes. This is not going to be an easy question to answer. Although the detection of intermediate dihydrogen complexes on the pathway to classical hydride products would represent an unambiguous answer, it may be in some cases that the proton merely approaches the metal along a trajectory which is close to the hydride ligands. In this latter case the proton–hydride interaction is much more fleeting and consequently this is a pathway which is much more difficult to identify. Certainly the use of rapid reaction techniques is essential in order to define the intimate mechanisms of these facile reactions.

References

1 D. J. Evans, R. A. Henderson and B. E. Smith, *Bioinorganic Catalysis*, ed. J. Reedijk, Marcel-Dekker, New York, 1993, 89.
2 K. E. Oglieve and R. A. Henderson, *J. Chem. Soc., Chem. Commun.*, 1993, 474 and refs. therein.
3 P. G. Jessop and R. H. Morris, *Coord. Chem. Rev.*, 1992, **121**, 155 and refs. therein.
4 R. H. Crabtree, G. G. Hlatky, C. P. Parnell, B. E. Segmüller and R. J. Uriate, *Inorg. Chem.*, 1984, **23**, 354.
5 F. M. Conroy-Lewis and S. J. Simpson, *J. Chem. Soc., Chem. Commun.*, 1987, 1675.
6 T. Arliguie, B. Chaudret, F. A. Jalon, A. Otero, J. Lopez and F. J. Lahoz, *Organometallics*, 1991, **10**, 1888.
7 G. Jia, A. J. Lough and R. H. Morris, *Organometallics*, 1992, **11**, 161.
8 K. E. Oglieve and R. A. Henderson, *J. Chem. Soc., Chem. Commun.*, 1992, 441.
9 N. D. Silavwe, M. P. Castellani and D. R. Tyler, *Inorg. Synth.*, 1992, **29**, 204.
10 M. L. H. Green and P. J. Knowles, *J. Chem. Soc., Perkin Trans. 1*, 1973, 989.
11 M. L. H. Green, J. A. McCleverty, L. Pratt and G. Wilkinson, *J. Chem. Soc. A*, 1961, 4854.
12 J. E. Bercaw, *Polyhedron*, 1988, **7**, 2053.
13 G. Parkin and J. E. Bercaw, *J. Chem. Soc., Chem. Commun.*, 1989, 255.
14 H. Werner, *Angew. Chem., Int. Ed. Engl.*, 1977, **16**, 1.
15 R. G. Wilkins, *Kinetics and Mechanism of Reactions of Transition Metal Complexes*, VCH, Weinheim, 2nd edn., 1991, pp. 33–37.
16 G. Jia and R. H. Morris, *Inorg. Chem.*, 1990, **29**, 582.
17 G. R. K. Khalsa, G. J. Kubas, C. J. Unkefer, L. S. Van Der Sluys and K. A. Kubat-Martin, *J. Am. Chem. Soc.*, 1990, **112**, 3855.
18 X-L. Luo and R. H. Crabtree, *J. Chem. Soc., Chem. Commun.*, 1990, 189.
19 M. T. Haward, M. W. George, P. Hamley and M. Poliakoff, *J. Chem. Soc., Chem. Commun.*, 1991, 1101.
20 X-L. Luo, D. Michos and R. H. Crabtree, *Organometallics*, 1992, **11**, 237.
21 K. Zhang, A. A. Gonzalez and C. D. Hoff, *J. Am. Chem. Soc.*, 1989, **111**, 3627.
22 G. J. Kubas, *Acc. Chem. Res.*, 1988, **21**, 120 and refs. therein.
23 P. J. Desrosiers, L. Cai, Z. Lin, R. Richards and J. Halpern, *J. Am. Chem. Soc.*, 1991, **113**, 4173 and refs. therein.
24 Ref. 15, p. 6.
25 J. M. Manriquez, P. J. Fagan and T. J. Marks, *J. Am. Chem. Soc.*, 1978, **100**, 3939.
26 C. R. S. M. Hampton, I. R. Butler, W. R. Cullen, B. R. James, J-P. Charland and J. Simpson, *Inorg. Chem.*, 1992, **31**, 5509.
27 R. J. Klingler, J. C. Huffman and J. K. Kochi, *J. Am. Chem. Soc.*, 1980, **102**, 208.
28 L. F. Rhodes, J. C. Huffman and K. G. Caulton, *Inorg. Chim. Acta*, 1992, **198–200**, 639.
29 S. P. Albracht, *J. Recl. Trav. Chim. Pays-Bas*, 1987, **106**, 173.
30 R. A. Henderson, *J. Chem. Soc., Chem. Commun.*, 1987, 1670 and refs. therein.

Received 28*th May* 1993; *Paper* 3/03048B